Quantum Amplified Isomerization: A New Concept for Polymeric Optical Materials[1]

J. G. Gillmore,[⊥,†] J. D. Neiser,[‡] K. A. McManus,[†] Y. Roh,[†] G. W. Dombrowski,[†] T. G. Brown,[*,‡] J. P. Dinnocenzo,[*,†] S. Farid,[*,§] and D. R. Robello[*,§]

Department of Chemistry, Center for Photoinduced Charge Transfer, University of Rochester, Rochester, New York 14627-0216; The Institute of Optics, University of Rochester, Rochester, New York 14627-0186; and Research Laboratories, Eastman Kodak Company, Rochester, New York 14650-2116

Received February 17, 2005; Revised Manuscript Received July 1, 2005

ABSTRACT: The preparation and evaluation of a new class of photoresponsive polymers are described on the basis of a process called quantum amplified isomerization (QAI). The QAI process utilizes photoinitiated, cation radical isomerization chemistry in a polymeric medium. Two classes of materials are described: one where the QAI reactant is molecularly doped in the polymer matrix and another where the reactant is part of a functionalized polymer. Quantum yield experiments demonstrate that the isomerization reaction can proceed by a chain process with modest efficiencies. Photochemical conversion experiments show that high extents of conversion of the QAI reactants are possible. The rate and extent of conversion are strongly correlated to the glass transition temperature of the polymer. For molecularly doped polymers, hypotheses to explain the high conversions based on diffusion or phase separation of the reactants were tested and excluded. Models are discussed to rationalize experimental factors that affect the quantum yields and the photochemical conversions.

Introduction

Photoinduced electron transfer (PET) reactions in rigid matrices form the basis of several technologically important processes. Of these, the most widely applied are silver halide photography and electrophotography, where electron transfer or charge transport occurs at an interface or in a heterogeneous medium.[2] PET processes between molecularly dissolved reactants in polymeric media are also well-known. Examples of the latter include the PET generation of free radicals or acids that can be used to initiate polymerizations[3] or induce other reactions, such as those used in photolithography.[4] In most of these processes amplification of the primary photochemical reaction is an important component. In silver halide photography and acid-induced chemical transformations, the photochemical process leads to the formation of a latent image, an entity that can be used in a subsequent treatment (development) as a catalyst to amplify the effect of the primary step. In photoinitiated polymerization the conversion of many monomeric units into a polymeric molecule is also a form of amplification.

Herein we describe a new class of photoresponsive materials based on photoinduced electron-transfer chain isomerizations in polymeric matrices. Photoinduced electron-transfer reactions in fluid media have long been demonstrated to have the potential for amplification by a chain mechanism.[5] These reactions usually take place in polar solvents such as acetonitrile, where free (i.e., fully separated) ion radicals can be formed. As shown in Scheme 1, chain reactions can occur when a reactant

Scheme 1

$$S \xrightarrow{h\nu} {}^1S^*$$

$${}^1S^* + R \longrightarrow S^{-\bullet} + R^{+\bullet}$$

$$R^{+\bullet} \longrightarrow P^{+\bullet}$$

$$P^{+\bullet} + R \longrightarrow P + R^{+\bullet}$$

cation radical ($R^{+\bullet}$) isomerizes to a product cation radical ($P^{+\bullet}$) that is capable of undergoing electron-transfer reaction with another R to form $R^{+\bullet}$. The latter process will be energetically favorable if the oxidation potential of P is greater than that of R. It is important to note that rapid diffusion is necessary for both initiation and propagation of the chain reaction.

We set out to determine the feasibility of photochemically initiated cation radical chain isomerization reactions in the restrictive environment of rigid polymer matrices. Scheme 2 illustrates the concept, which we refer to as quantum amplified isomerization (QAI).[6] It is important to point out that, unlike ion radical chain reactions in polar solvents where diffusion and solvation of ion radicals occur readily, the high viscosity and the relatively low solvating power of polymers seemed likely to limit the extent of chain propagation in polymeric media since, as described above, diffusional processes are required in fluid media with these types of reactions for chain initiation and propagation. In addition, since diffusional separation of $S^{-\bullet}R^{+\bullet}$ ion radical pairs would also be severely impaired in polymer matrices, it seemed probable that chain-terminating return electron transfer to regenerate S and R might be a dominant process. Despite these potential difficulties, we recognized that if it was possible to achieve ion radical chain isomerizations in polymers—even with modest efficiencies—the resulting materials could have novel photoresponsive properties.

When assessing the potential for achieving ion radical chain isomerizations in a polymeric matrix, it is instruc-

† Department of Chemistry, University of Rochester.
‡ The Institute of Optics, University of Rochester.
§ Eastman Kodak Company.
⊥ Current address: Department of Chemistry, Hope College, Holland, MI 49424.
* Corresponding authors. E-mail: brown@optics.rochester.edu (T.G.B.); jpd@chem.rochester.edu (J.P.D.); samir.farid@kodak.com (S.F.); douglas.robello@kodak.com (D.R.R.).

10.1021/ma050348k CCC: $30.25
Published on Web 08/16/2005

Scheme 2

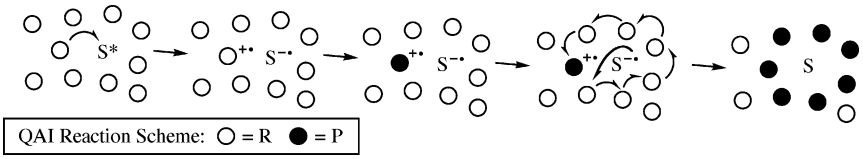

Scheme 3

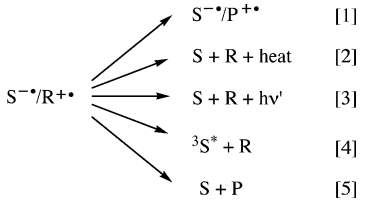

tive to consider the possible fates of geminate ion radical pairs produced by PET in low-polarity solvents where out-of-cage diffusion is not a dominant reaction. As shown in Scheme 3, there are several processes to consider: (1) adiabatic isomerization of the reactant cation radical to a product cation radical, (2) nonradiative return electron transfer, (3) radiative return electron transfer (i.e., exciplex fluorescence), (4) intersystem crossing to form the triplet excited state of the sensitizer (or the reactant), and (5) bond-coupled return electron transfer, a process that yields the neutral isomerization product. Of the reactions shown in Scheme 3, only adiabatic isomerization (reaction 1) has the potential for chain propagation, where interception of $S^{-\bullet}/P^{+\bullet}$ by a reactant molecule leads to $S^{-\bullet}/R^{+\bullet}$; all other reactions are chain-termination steps.

Results

Molecularly Doped Polymers. Adiabatic isomerization within the primary ion radical pair (reaction 1 in Scheme 3) is reported to be the dominant process for reaction of cage compound **1** with the singlet excited state of 9,10-dicyanoanthracene (DCA) in nonpolar solvents.[7] Thus, **1**/DCA seemed to be an ideal reactant/sensitizer pair to initially test the potential of initiating a cation radical chain isomerization in a polymer matrix.

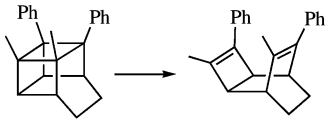

1 **2**

Poly(methyl methacrylate) (PMMA) films (≈20 μm) containing dissolved **1** and 0.01 M DCA were prepared on poly(ethylene terephthalate) sheets. The films were irradiated with uniformly intense light from a Hg arc lamp at 405 nm, where DCA selectively absorbs. Following irradiation, known areas of the irradiated films were dissolved in CH_2Cl_2 containing an internal standard. After precipitation of the PMMA, the filtered solutions were analyzed by HPLC to quantify the number of molecules of **2** that were formed. Experiments conducted with films containing 0.1 and 0.5 M **1** resulted in isomerization quantum yields, corrected for incomplete interception of the excited sensitizer, of 1.6 and 2.2, respectively. As shown in Table 1, upon further increases in reactant concentration and changes in the sensitizer structure, corrected quantum yields in the range of 4−5 were obtained for the isomerization reaction, consistent with a chain isomerization process.

Table 1. Quantum Yields for Isomerization of 1 and 3 in Polymeric Media

reactant	[reactant]	sensitizer[a]	ϕ_{isom}[b]
1	0.1	DCA	1.6
1	0.5	DCA	2.2
1	0.5	2-Bu^t-DCA	3.2
1	0.5	2,6-diBu^t-DCA	4.2
1	2.0	2,6-diBu^t-DCA	5.3
3	0.1	DCA	0.4
3	0.5	DCA	0.6
3	0.5	NMQ	1.2

[a] 0.02 M sensitizer. DCA = 9,10-dicyanoanthracene; 2-Bu^t-DCA = 2-*tert*-butyl-9,10-dicyanoanthracene; 2,6-diBu^t-DCA = 2,6-di(*tert*-butyl)-9,10-dicyanoanthracene; NMQ = *N*-methylquinolinium hexafluorophosphate. [b] Isomerization quantum yields were recorded at low conversion and were corrected for incomplete interception of sensitizer excited states.

Because compound **1** is somewhat thermally labile,[8] we considered the possibility that its isomerization may have been triggered by heat dissipation during the photoreaction. To test this hypothesis, PMMA films of **1** were prepared containing ferrocene in place of DCA. The excited state of ferrocene is incapable of oxidizing **1**, and upon photoexcitation, ferrocene is known to undergo rapid nonradiative decay to its ground state with high efficiency.[9] Therefore, photolysis of PMMA films containing ferrocene and **1** should convert all of the absorbed light energy into heat, thus providing an appropriate control experiment to determine whether sample heating could be the cause of isomerization of the **1** with DCA and the other electron-transfer sensitizers. In practice, 405 nm irradiation of films containing 0.5 M **1** and 0.6 M ferrocene resulted in no detectable isomerization, even after long irradiation times. This experiment rules out photochemical heating as an explanation for the photoinduced isomerization of **1** in PMMA. Nonetheless, the relatively low thermal stability of compound **1** prompted us to investigate other cation radical chain isomerizations in polymers.

Photoinduced electron-transfer isomerization of hexamethyl Dewar benzene (**3**) in polar solvents is known to lead to hexamethylbenzene (**4**) via a cation radical chain mechanism.[5a] It is also known that isomerization within the primary ion radical pair can occur in low-polarity solvents.[10] In nonpolar solvents, however, chain-propagating isomerization of $\mathbf{3}^{+\bullet}$ to $\mathbf{4}^{+\bullet}$ principally competes with bond-coupled return electron transfer (reaction 5 in Scheme 3), which is a chain-terminating reaction.[10,11] Although the latter reaction would lower the chain length for isomerization of **3** to **4**, the higher thermal stability of **3** and the ease of synthesizing functionalized derivatives offered major advantages over **1** to probe photoresponsive polymers based on QAI.

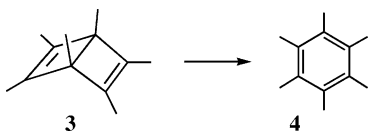

3 **4**

In practice, the quantum yield for isomerization of **3**/DCA in PMMA was lower than that for the isomer-

ization of **1** by a factor of ca. 4 (see Table 1). As found for **1**, the quantum yield for isomerization of **3** increased slightly with increasing reactant concentration. The corrected isomerization quantum yield for **3** was also found to increase when DCA was replaced by the cationic sensitizer *N*-methylquinolinium hexafluorophosphate (NMQ). These results will be discussed later.

Importantly, PMMA films containing **1** or **3** and DCA showed substantial, although incomplete, conversion upon irradiation, ≈75% and ≈45%, respectively. If the reactants are assumed to be uniformly distributed in the polymeric media, it is possible to estimate the charge separation distances between $DCA^{-\bullet}$ and $\mathbf{1}^{+\bullet}$ or $\mathbf{3}^{+\bullet}$ that would be required to account for the maximal conversions. On the basis of the DCA concentration of 0.01 M, the average separation distance between sensitizer molecules is ≈70 Å. To account for ≈75% conversion of **1**, a charge separation distance of ≈32 Å would be required. The extent of conversion of **3** (≈45%) requires a charge separation distance of ≈27 Å. Such separation distances are noteworthy given the low dielectric of the polymer medium.

We considered two alternative hypotheses that could explain the relatively high conversions of **1** and **3**: (i) diffusion and (ii) phase separation. Diffusion of the reactants during irradiation would obviate the need for long-distance charge separation. Similarly, phase separation of the reactants would provide high local concentrations of **1** or **3** in the polymer, which would reduce the extent of charge separation required for high conversion.

Estimates of the diffusion coefficients of the reactants in PMMA were needed to test the diffusion hypothesis. These were obtained from a forced Rayleigh scattering (FRS) experiment performed by holographic exposure.[12] A 20 μm thick coating on glass containing 0.5 M **3** and 0.010 M DCA in PMMA was irradiated by using two equal-intensity 407 nm laser beams that were crossed at an angle of 35.55° normal to the film plane. The resulting periodic spatial modulation of **3** and its isomerization product, **4**, gave rise to a diffraction grating with a period of 350 nm. The strength of the grating was measured by using 633 nm light from a HeNe laser incident at the angle appropriate to satisfy the Bragg condition. Long-term monitoring of the grating showed a gradual drop in the diffraction efficiency of 10% over 20 days. If all of this decrease in diffraction efficiency is attributed to diffusion, the resulting diffusion coefficient (D) is calculated to be $\approx 9 \times 10^{-19}$ cm^2/s.[13] On the basis of the similar molecular volumes of **3** (252 Å^3) and DCA (269 Å^3),[14] it is reasonable to assume that they will have similar diffusion coefficients. These diffusion coefficients can be used to test the diffusion model in eq 6, where S is the sensitizer (DCA in this case), R is the reactant (**1** or **3**), and P is the isomerization product (**2** or **4**).

$$\mathrm{S} + \mathrm{R} \underset{k_{-\mathrm{diff}}}{\overset{k_{\mathrm{diff}}}{\rightleftharpoons}} \mathrm{S/R} \xrightarrow[k_{\mathrm{rxn}}]{h\nu} \mathrm{S/P} \qquad (6)$$

The rate constants for diffusion of **3** and DCA in PMMA (k_{diff}) were estimated by using the Smoluchowski equation, eq 7.[15] The sum of the diffusion coefficients (D_{ab}) for **3** and DCA was approximated as twice the diffusion coefficient measured for **3** in PMMA. The encounter radius (r_{ab}) was estimated to be 10 Å, which is ca. 2 Å greater than the sum of the average molecular radii of **3** (3.9 Å) and DCA (4.0 Å). This estimate for r_{ab} assumes that electron transfer from **3** to DCA* can occur at distances that are slightly larger than van der Waals contact. The calculated value for k_{diff} based on the above estimates is $\approx 1.4 \times 10^{-3}$ M^{-1} s^{-1}.

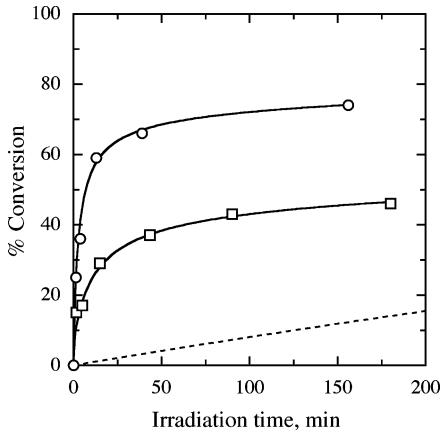

Figure 1. Photochemical conversion experiments with 0.5 M **1** (circles) or **3** (squares) in PMMA containing 0.01 M DCA using 407 nm laser. Interpolated lines are drawn through the experimental data points. The dashed line shows predicted conversion for **3** based on the diffusion model (see text); this line neglects the small extent of prompt conversion (<2%) due to static quenching of the sensitizer.

$$k_{\mathrm{diff}} = 4\pi r_{\mathrm{ab}} D_{\mathrm{ab}} N_{\mathrm{A}} \qquad (7)$$

The magnitudes of the rate constant for diffusional separation of the S/R pair ($k_{-\mathrm{diff}}$) and for the DCA-photosensitized isomerization of DCA/**3** in PMMA (k_{rxn}) were needed to determine which step in the kinetic scheme would be rate limiting. The value of $k_{-\mathrm{diff}}$ can be determined from k_{diff} and the effective equilibrium constant for formation of the encounter pair DCA/**3** that leads to quenching of DCA* ($K = k_{\mathrm{diff}}/k_{-\mathrm{diff}}$). The equilibrium constant can be directly measured from fluorescence quenching. Steady-state fluorescence experiments show that ≈2/3 of the DCA excited states are quenched by 0.5 M **3** in PMMA. Thus, $K \approx 4$ M^{-1}, which when combined with k_{diff} gives $k_{-\mathrm{diff}} \approx 3.5 \times 10^{-4}$ s^{-1}. The value of k_{rxn} can be determined from the photon flux, the number of molecules of DCA in the exposed region of polymer film, and the fraction of light absorbed. Combining these experimental quantities gives $k_{\mathrm{rxn}} = 1.6$ photons absorbed per DCA molecule per second. Because $k_{-\mathrm{diff}} \ll k_{\mathrm{rxn}}$, essentially every excited DCA/**3** pair undergoes photoreaction before diffusional separation can occur. This requires that diffusional encounter of **3** and DCA be rate limiting for the hypothetical kinetic scheme shown in eq 6. Since DCA is not consumed in the photoisomerization reaction, the concentration of DCA remains constant. Therefore, the rate constant for diffusion (and isomerization) should obey simple first-order kinetics, where the observed rate constant is equal to k_{diff} [DCA], or 1.4×10^{-5} s^{-1}. This rate constant was used to predict the conversion vs irradiation time for photosensitized isomerization of **3** with DCA for a diffusional process (see dashed line in Figure 1). The data clearly show that the diffusion model is kinetically incompetent to explain the DCA-photosensitized conversion of **3** to **4** in PMMA.

It was not possible to determine the diffusion coefficient for **1** in PMMA by FRS because of the slow thermal isomerization of **1** to **2** over extended time periods. However, on the basis of the larger molecular

volume of **1** (416 Å^3) vs **3** (252 Å^3), it is expected that $D(\mathbf{1}) \ll D(\mathbf{3})$.[16] **1** undergoes isomerization even more rapidly than **3**; therefore, diffusion is clearly kinetically incompetent to explain the observed DCA-photosensitized conversion of **1** to **2** in PMMA. Finally, in addition to the quantitative arguments against diffusion for **1** and **3**, we note that the diffusion model predicts that the extent of conversion to product should exhibit an exponential dependence on irradiation time that leads to complete isomerization of the reactants, which is not observed experimentally.

Having excluded diffusion as a hypothesis to explain the high rates and extents of conversions for **1** and **3** in polymeric media, we next sought to test whether phase separation could rationalize the conversion data. To test for phase separation, PMMA films containing **1** or **3** were analyzed by transmission electron microscopy (TEM). TEM images of PMMA samples containing no additive or containing **1** at concentrations of 0.5 and of 2.0 M were indistinguishable, even at 50 000-fold magnification. Similarly, no evidence for phase separation was found for PMMA films containing **3** at 0.5 M. Only at high concentrations of **3** (1.5−2.0 M) in PMMA was phase separation evident by films that were visually cloudy.

Although the TEM experiments unambiguously rule out phase separation on length scales of >20 nm, they cannot exclude phase separation on significantly smaller length scales. Therefore, to more critically test the phase separation hypothesis, we prepared polymers in which the QAI reactants were covalently attached to the polymer backbone. The goal was to determine whether functionalized polymers—in which both phase separation and diffusion are prohibited—behaved similarly to the molecularly doped systems described above with respect to the QAI process.

Functionalized Polymers. Functionalized polymers were prepared with a Dewar benzene moiety rather than the cage compound (**1**) because of the relative ease of synthesis of Dewar benzene derivatives as well as their thermal stability. Methacrylic monomer **5** (DBMA) was chosen as a target monomer for conventional free radical polymerization.

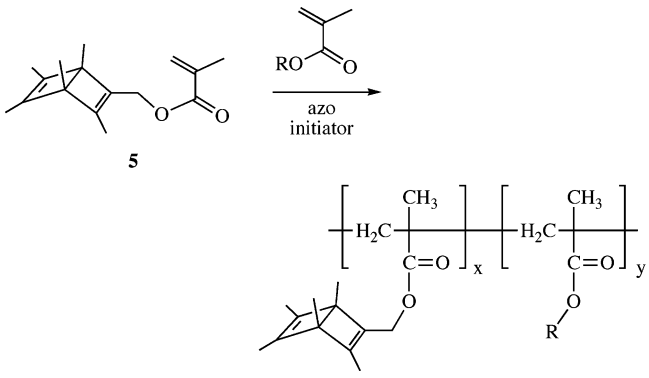

Before embarking on the synthesis of **5**, the feasibility of free radical polymerization in the presence of hexamethyl Dewar benzene (**3**) was performed to test whether possible chain transfer reactions involving the allylic hydrogen abstraction from the Dewar benzene moiety might interfere with the polymerization. A bulk polymerization of methyl methacrylate (MMA) using the conventional free radical initiator azobis(isobutyronitrile) (AIBN), and in the absence and presence of **3** (17 mol %), was carried out. The isolated polymers for the samples prepared with and without added **3** were found to have similar yields, molar mass distributions, and glass transition temperatures. Moreover, **3** was recovered quantitatively after the polymerization. These results indicated that **3** did not interfere with the free radical polymerization and that similar polymerization of **5** should be feasible.

The synthesis of Dewar benzene-substituted monomer **5** is shown below. Ethyl ester **6** was prepared by the method previously reported for the analogous methyl ester.[17] Reduction of **6** with diisobutylaluminum hydride (DIBAL-H) provided alcohol **7**, which was subsequently esterified with methacryloyl chloride to give **5**.

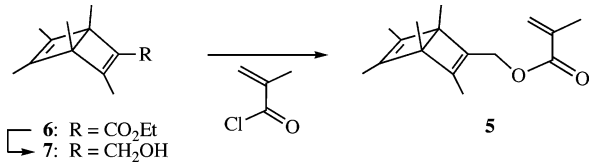

Monomer **5** was successfully copolymerized with varying relative amounts of methyl methacrylate, *n*-hexyl methacrylate, or cyclohexyl methacrylate. Copolymers containing high concentrations of the Dewar benzene-derived repeat units (>50 mol %) tended to yellow and became insoluble upon storage at room temperature over a period of days to weeks, which is due to an, as yet, unidentified cross-linking reaction. However, copolymers more dilute in Dewar benzene moieties were found to be stable for long periods of time. We concentrated our studies on copolymers containing approximately 10 mol % of Dewar benzene repeat units. These samples remained colorless and soluble throughout the course of our experiments. In addition, the concentration of Dewar benzene moieties in the 10% copolymers is somewhat similar to those employed in experiments in which **3** was molecularly doped into host polymers. We presume that the distributions of repeat units in the copolymers were random because reactivity ratios of nearly all simple, alkyl methacrylates are close to unity.[18]

Photoinduced isomerizations were first studied with copolymers prepared from Dewar benzene monomer **5** and methyl methacrylate, p(DBMA/MMA), and from **5** and *n*-hexyl methacrylate, p(DBMA/HMA). Polymer films containing sensitizer were coated on poly(ethylene terephthalate) sheets and irradiated at 405 nm, as described above. After dissolution of the polymer films in $CDCl_3$, the extent of isomerization of the Dewar benzene to benzene moieties was assessed by integration of the ester α-methylene ^{1}H NMR resonances of the reactant vs product moieties. The ratio of the α-methylene integrals vs the α-ester proton resonances from the comonomer was nearly constant (within 10%) as a function of photochemical conversion, consistent with a clean isomerization reaction for the functionalized polymers. Conversion experiments with p(DBMA/MMA) and p(DBMA/HMA) containing DCA showed significant differences (see Figure 2). Interestingly, the limiting conversion for p(DBMA/MMA) is less than one-half that observed for **3** dissolved in PMMA. These results are discussed below.

One obvious difference between p(DBMA/MMA) and p(DBMA/HMA) is their glass transition temperatures, 115° vs 4°, respectively. To test whether varying T_g could be the cause of the contrasting conversion results in Figure 2, the photochemical conversion of p(DBMA/

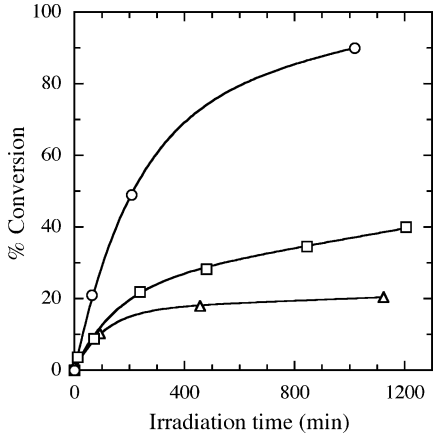

Figure 2. Photochemical conversion experiments with p(DBMA/HMA) (circles), p(DBMA/cHMA) (squares), and p(DBMA/MMA) (triangles) containing ≈0.01 M DCA using a Hg arc lamp. Interpolated lines are drawn through the experimental data points.

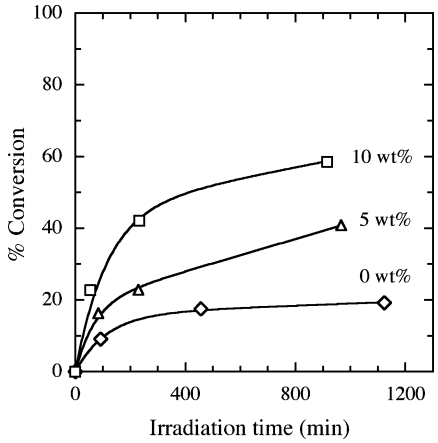

Figure 3. Photochemical conversion of p(DBMA/MMA)/DCA with various weight percentages of plasticizer (di-*n*-butyl phthalate). Interpolated lines are drawn through the experimental data points.

MMA) was studied with 0, 5, and 10 wt % of an added plasticizer, dibutyl phthalate (DBP). The T_gs of these film compositions were estimated to be 115, 89, and 65 °C, respectively.[19] As shown in Figure 3, increasing amounts of DBP in films of p(DBMA/MMA) lead to increasing conversion. These results with plasticized polymers, as well as the results with unplasticized, functionalized polymers, are consistent with T_g playing an important role in controlling the limiting extent of conversion. Interestingly, the estimated T_g of the film containing 5 wt % DBP (89 °C) is reasonably similar to that determined for 0.5 M **3** in PMMA (95 °C), as are their extents of conversion, ≈40% and ≈45%, respectively. These data suggest that the higher limiting conversion found for **3** dissolved in PMMA vs the unplasticized, functionalized polymer p(DBMA/MMA) is due to the plasticizing effect of **3** in the former system, which decreases the T_g of the molecularly doped polymer and thereby increases the ultimate conversion.

Conversions were also compared for p(DBMA/HMA) and the copolymer of **5** with cyclohexyl methacrylate, p(DBMA/cHMA). Although these two copolymers are expected to have reasonably similar polarities, they have significantly different T_gs (4 vs 104 °C). The maximal extent of conversion for p(DBMA/cHMA) was found to be ≈40%, much lower than that observed for p(DBMA/HMA), ≈90%, but similar to that found for p(DBMA/MMA) (see Figure 2). These data again point to T_g being an important factor controlling the extent of conversion.

Overall, the combined conversion experiments show that molecularly doped and functionalized QAI polymer systems behave similarly with regard to extent of conversion, so long as systems of similar T_g are compared. We next sought to compare molecularly doped vs functionalized polymer systems in terms of their relative quantum yields for isomerization.

Unlike the conversion experiments, quantum yield experiments with molecularly doped polymers showed that T_g did not substantially affect the reaction quantum yields, presumably because the quantum yields are measured at low conversion of the reactants. For example, the isomerization quantum yields for **1** in PMMA and poly(*n*-butyl methacrylate) were indistinguishable within experimental error. Isomerization quantum yields for the functionalized polymers were, nevertheless, measured with plasticized samples to provide a closer comparison to the molecularly doped systems. Quantum yields for p(DBMA/MMA) and 0.5 M **3** in PMMA were compared with both DCA and NMQ as photosensitizers. For DCA, the quantum yields were 0.3 and 0.6 for functionalized and molecularly doped QAI polymers, respectively. With NMQ, the respective quantum yields were 1.0 and 1.2. Overall, the quantum yields for functionalized and molecularly doped QAI polymers are quite similar. The slightly lower quantum yields observed for the functionalized polymer may be attributable to the necessity of carrying the reactions to higher conversions to obtain acceptable signal-to-noise for the analytical method employed (^{1}H NMR vs GC). The quantum yield differences are rather small, however, and suggest that the molecularly doped QAI polymers and the functionalized polymers behave similarly.

Finally, although diffusion in functionalized polymers was expected to be slow, a forced Rayleigh scattering experiment was conducted to test this prediction. As described above, a weak diffraction grating was written with a 350 nm period in p(DBMA/MMA) containing DCA and 20 wt % plasticizer. Long-term monitoring of the grating showed negligible loss (<0.03%) in its diffraction efficiency over 23 days, demonstrating negligible diffusion of the polymer chains in the functionalized polymer, even when heavily plasticized.

Discussion

The experiments described above provide the first test of the QAI concept for polymeric materials based on electron-transfer-initiated, ion radical chain isomerization. The results show that isomerization quantum yields can exceed unity, although the chain amplification is significantly lower than that observed in polar, fluid solution. Even when the quantum yield is <1, as for some cases with the isomerization of **3** to **4**, chain amplification is nonetheless evidenced by the fact that the isomerization quantum yield, corrected for incomplete interception of the excited sensitizer, increases with increasing reactant concentration. That the quantum yields for the QAI reactions are lower in polymeric media than in polar solvents is not surprising. In polar, fluid solvents, diffusive separation of the sensitizer anion radical and the substrate cation radical in the geminate ion radical pair can readily occur. Ion radical separation naturally leads to a diminished rate for

chain-terminating return electron transfer and consequently greater isomerization quantum yields. Similarly, chain-propagating electron transfer from the neutral QAI reactant to the product cation radical is enhanced in fluid solution by a diffusional process. As demonstrated by the forced Rayleigh scattering experiments, neither of these chain-propagating processes can occur rapidly in a rigid polymer medium due to the low rate constants for diffusion. In addition, the polymer matrix may inhibit the chain isomerization process in more subtle ways. For example, the rigid polymer medium may sterically constrain isomerization of the reactant cation radicals, thereby allowing chain-terminating return electron transfer to more effectively compete. In addition, the rigid nature of the polymer makes it intrinsically nonpolar. This makes chain propagation more difficult in a polymer because, in the absence of molecular diffusion, propagation requires charge separation of the sensitizer anion radical and the chain-propagating cation radicals. Given the above obstacles to ion radical chain isomerizations in polymer hosts, it is remarkable that the reactions proceed at all beyond the contact ion radical pair stage.

Quantum Yields. The rigid polymer medium clearly restricts diffusion of QAI reactants and products in the matrix; therefore, it is of interest to consider how the isomerization proceeds under these constraints. We begin with the reaction of bishomocubane **1** with DCA in polymer. Because diffusion is negligible in the polymer medium, fluorescence quenching of the singlet excited state of DCA by **1** must occur by static quenching. Static quenching is commonly interpreted according to the Perrin model,[20] eq 8, where ϕ_0 and ϕ are the integrated fluorescence intensities in the absence and presence of quencher. The average number of quenchers in the quenching sphere (λ_Q) is equal to $VN_A[Q]$, where V is the volume that contains effective quenchers, N_A is Avogadro's number, and [Q] is the quencher concentration. For 0.5 M **1** in polymer, ϕ_0/ϕ was 2.0, from which V was determined to be ≈2240 Å^3.[21] This corresponds to a quenching sphere with an average radius of ≈8 Å. The average numbers of molecules within the 8 Å quenching sphere (λ_Q) are 0.14 and 0.69 for 0.1 and 0.5 M **1**, respectively.

$$\ln(\phi_0/\phi) = \lambda_Q = VN_A[Q] \tag{8}$$

The quantum yields measured at 0.1 and 0.5 M **1** are 1.6 and 2.2, respectively. On the basis of photochemical measurements in nonpolar fluid media, the geminate ion pair DCA$^{-\bullet}$/**1**$^{+\bullet}$ undergoes adiabatic isomerization to DCA$^{-\bullet}$/**2**$^{+\bullet}$ with essentially unit efficiency. Assuming this phenomenon holds in the polymeric matrix, the amplification due to chain propagation would be 0.6 and 1.2, respectively. Thus, as the concentration of **1** increases by a factor of 5, chain propagation increases only by a factor of 2. This suggests that the amplification is proportionally more effective at lower concentration, which is consistent with a larger propagation distance at low concentration.

The average distance of chain propagation required by the isomerization quantum yields (ϕ_{isom}) can be estimated by using eq 9, where λ_R is the average, initial number of reactant molecules in the reaction sphere, λ_S is the average number of molecules in the shell that lies outside the quenching sphere but inside the reaction sphere, and f_q is the fraction of excited-state DCA molecules that are quenched by **1**. Because not all reaction spheres contain a reactant molecule within their enclosed quenching spheres, the λ_S term must be multiplied by $P_Q(0)$, the probability that a quenching sphere contains no quencher. $P_Q(0)$ is equal to $\exp(-\lambda_Q)$.[20] Making this substitution into eq 9, and noting that $\lambda_S = \lambda_R - \lambda_Q$, gives eq 10.

$$\phi_{isom} = \{\lambda_R - \lambda_S P_Q(0)\}/f_q \tag{9}$$

$$\phi_{isom} = \{\lambda_R - (\lambda_R - \lambda_Q)\exp(-\lambda_Q)\}/f_q \tag{10}$$

The reaction sphere for DCA/**1** upon initial excitation can be calculated using eq 10 and the experimental values for ϕ_{isom}, λ_Q, and f_q. The calculated values for λ_R at 0.5 and 0.1 M **1** are 1.87 and 1.89, respectively. These values can be used to determine the average chain propagation volumes and radii via eq 8 by substituting λ_R for λ_Q. Within the framework of this reaction sphere model, the average chain propagation radii are ≈20 and ≈11 Å at 0.1 and 0.5 M **1**, respectively. These results are consistent with the qualitative conclusion made above, namely that a larger fraction of chain propagation occurs outside the quenching sphere at lower reactant concentration.

A possible explanation for the greater chain propagation distance at lower reactant concentration can be inferred from the reaction quantum yield dependence on the concentration of **1**. The fact that the quantum yields do not increase in direct proportion to [**1**] suggests that the ion radical chain initiation efficiency decreases, or termination increases, or both, as the reactant concentration increases. The effect of concentration on the efficiencies of chain initiation/termination can be plausibly related to the separation distance between the geminate ion radical pairs formed upon initial photoinduced electron transfer from **1** to the excited state of DCA. At high concentration of **1**, a greater fraction of sensitizers will have a reactant molecule in contact with the sensitizer, which will lead to the formation of "contact" or "tight" ion radical pairs. In contrast, at low concentration of **1**, a greater fraction of "separated" or "loose", geminate ion radical pairs will be formed. We propose that the changes in the relative proportion of contact vs separated, geminate ion radical pairs might result in differential efficiencies of chain initiation and termination. The analysis begins by first understanding that the chain propagation step involving electron transfer from **1** to DCA$^{-\bullet}$/**2**$^{+\bullet}$ will, in general, require some charge separation for both contact and separated geminate ion radical pairs. Because of an inverse dependence on ion radical pair separation distance, the Coulombic barrier for charge separation will be larger for contact geminate ion radicals pairs than for separated ones. Consequently, chain-terminating return electron transfer for contact, geminate ion radical pairs will more effectively compete with chain propagation than for separated, geminate pairs. This would explain why ϕ_{isom} does not increase in direct proportion to [**1**]. The preceding analysis leads to several important conclusions. First, it suggests that increasing the reactant concentration to increase ϕ_{isom} will yield diminishing returns because higher substrate concentrations will necessarily increase the fraction of contact ion radical pairs, which are less efficient at chain initiation. In addition, the model suggests that a more effective strategy for increasing ϕ_{isom} would be to use sterically encumbered sensitizers that prevent "contact" geminate

ion radical pairs from being formed. This is a potentially fruitful direction for future research on electron-transfer-based QAI materials.

In contrast to the results with DCA and **1**, a somewhat different picture emerges for the isomerization of Dewar benzene **3** with DCA as sensitizer. The values of λ_Q from fluorescence quenching experiments are calculated to be ≈0.3 at 0.1 M and ≈1 at 0.5 M **3**. The experimental isomerization quantum yields are 0.4 and 0.6, respectively. A comparison of the λ_Q and ϕ_{isom} values show that the initial-reaction spheres for **3** are, on average, comparable to or smaller than the fluorescence quenching spheres. Although the quantum yield does increase with increasing [**3**], suggesting that chain isomerization does occur, the reaction is significantly less efficient than for **1**. The lower efficiency for isomerization of **3** could have several origins. For example, the isomerization of **3** to **4** might proceed by an intrinsically less efficient cation radical chain reaction than for **1** to **2**. Quantum yields in fluid solution suggest just the opposite is true, however.[22] Therefore, a more likely explanation is that the cation radical chain isomerization of **3** suffers from a chain termination process that **1** does not. Solution studies of **3** and DCA in a nonpolar solvent have shown that the predominant decay process of the $DCA^{-\bullet}/\mathbf{3}^{+\bullet}$ geminate ion radical pair is return electron transfer to neutral **3**.[11] In contrast, the $DCA^{-\bullet}/\mathbf{1}^{+\bullet}$ exciplex is known to undergo adiabatic isomerization to $DCA^{-\bullet}/\mathbf{2}^{+\bullet}$ with unit efficiency in nonpolar solvent.[7] Similar behavior in PMMA would explain the lower isomerization quantum yields for **3** vs **1**.

Finally, we note that the isomerization quantum yields for **1** and **3** in polymeric media depend on the structure of the sensitizer. For **1**, the quantum yields were found to increase along the series DCA, 2-*tert*-butyl-DCA (BDCA), and 2,6-di-*tert*-butyl-DCA (DBDCA). This trend can be rationalized in terms of the expected rate constants for chain-terminating return electron transfer. The return electron transfers are highly exothermic for all of these sensitizers and should lie in the Marcus inverted region. On the basis of the reduction potentials for DCA (−0.91), BDCA (−0.95), and DBDCA (−0.99 V vs SCE), return electron transfer will be least exothermic for DCA and most exothermic for DBDCA. Consequently, the rate constants for return electron transfer are expected to decrease from DCA to BDCA to DBDCA. Thus, the increase in corrected quantum yields is most likely due to the differences in reaction energetics for return electron transfer, although a contribution from modest steric crowding might play a minor role.

The isomerization quantum yield for **3** in polymer was found to be higher with *N*-methylquinolinium hexafluorophosphate (NMQ) than with DCA as a sensitizer (1.2 vs 0.6; see Table 1). The reduction potential for NMQ is less negative than that for DCA (−0.85 vs −0.91 V vs SCE), which would be expected to increase the rate constant for return electron transfer for NMQ and lead to lower quantum yield.[23] At present, the cause of the greater quantum yield for NMQ is not clear; one possibility is that the partitioning between return electron transfer and isomerization of the geminate ion radical pairs differs for the positively charged and neutral sensitizers.

Conversion Studies. As discussed above, the conversion of significant numbers of reactant molecules outside the quenching sphere requires charge separation between the sensitizer anion radical and the reactant/product cation radicals. Consistent with this expectation, the conversion studies for both molecularly doped and functionalized polymers show that the isomerization quantum yields decrease dramatically with increased conversion.

The glass transition temperature (T_g) of the polymer medium had a significant effect on the quantum yield and ultimate extent of conversion. We interpret this observation in terms of the ability of the medium to accommodate chain-propagating charge separation. With functionalized QAI polymers, the T_g was changed either by altering the polymer structure or by the addition of plasticizers. An instructive example in the former category is the comparison of p(DBMA/HMA) and p(DBMA/cHMA). These two polymers contain similar alkyl ester groups but have quite different T_gs. The *n*-hexyl methacrylate polymer, which has the lower T_g, shows much higher overall conversion upon prolonged irradiation (Figure 2), suggesting that the polymer is better able to accommodate charge separation. This can be attributed to increased segmental mobility of the polymer chains, which increases the effective solvating ability of the polymer.

When the T_g is lowered by the addition of plasticizers, there is a similar effect on the quantum yield and overall extent of conversion (Figure 3). In this case, the cause of the effect is less clear. The added plasticizer could increase the polarity of the medium by either increasing the polymer chain mobility or by increasing the average polarity of the medium. Although our experiments do not distinguish between these possibilities, studies with solvatochromic dyes in methacrylate polymers have shown that the addition of plasticizers principally increases polarity by increasing polymer chain motion.[24]

The effect of T_g on reaction efficiency also provides an explanation for the higher conversion observed when **3** is molecularly doped into PMMA, rather than when the Dewar benzene is incorporated into a functionalized polymer (compare Figures 1 and 3). When **3** is added as a dopant, it acts to plasticize the polymer medium and thereby leads to an increase in the extent of conversion. When molecularly doped and functionalized polymers of similar T_g are compared, the extents of conversions are similar. It is worth noting that the plasticizers used for the functionalized polymers—phthalate esters—are significantly more polar than **3**. This provides preliminary evidence that the plasticizers principally increase the polarity of the polymer medium by increasing polymer chain mobility rather than by increasing the average polarity by dilution with a polar dopant.

Finally, that **1** is capable of achieving a greater overall conversion than **3**, upon prolonged irradiation in polymeric media, is consistent with the greater isomerization quantum yields for **1**. As discussed above, chain-terminating return electron transfer is less prevalent for **1**; consequently, chain initiation is more efficient for **1** than for **3**.

Experimental Section

Materials. Dichloromethane was distilled from phosphorus pentoxide under nitrogen and stored over anhydrous sodium carbonate prior to use. Ether was purified by passing the solvent over a bed of activated alumina.[25] Hexamethyl Dewar benzene (**3**) was fractionally distilled from lithium aluminum hydride through a glass helices-packed column at reduced pressure (bp 47 °C, 17 mmHg). Bis(3-*tert*-butyl-4-hydroxy-5-

methylphenyl) sulfide was a gift from Kodak Research Laboratories and used as received. Methacryloyl chloride was purified immediately before use by fractional distillation at atmospheric pressure from a few milligrams of bis(3-*tert*-butyl-4-hydroxy-5-methylphenyl) sulfide. Triethylamine was distilled from calcium hydride at atmospheric pressure under nitrogen before use. Compound **1** was prepared by a literature procedure.[7b] Poly(methyl methacrylate) (PMMA) was obtained from Polysciences (M_w = 25 000, T_g = 119 °C) and was used as received. 2,2′-Azobis(isovaleronitrile) (Vazo-67) was purified by recrystallization from boiling ligroin. 1,3,5-Trioxane was sublimed before use. 9,10-Dicyanoanthracene (DCA) was recrystallized twice from boiling pyridine and once from boiling acetonitrile. 2-*tert*-Butyl-9,10-dicyanoanthracene (BDCA) and 2,6-di-*tert*-butyl-9,10-dicyanoanthracene (DBDCA) were gifts from Kodak Research Laboratories and were used as received. *N*-Methylquinolinium hexafluorophosphate (NMQ) was prepared by a literature procedure.[26] Poly(ethylene terephthalate) film backing (ESTAR Base) was a gift from Kodak Research Laboratories and was used as received. The dimensions of the ESTAR Base were 100 μm thick × 5 in. wide. The ESTAR Base was coated with a thin (<0.5 μm) layer of latex (15/79/6 acrylonitrile/vinylidene chloride/acrylic acid) to improve coating adhesion. All other materials were commercially available and used as received.

Instrumentation. All laboratory operations with polymer film samples were performed under yellow lights. ^{1}H NMR spectra were recorded on 400 MHz spectrometers equipped with either a quad nuclear probe or a broadband proton X probe. UV−vis spectra were recorded on a diode array spectrophotometer. High-resolution mass spectrometry was performed on a JEOL HX-110 mass spectrometer operated at 10 000 resolution (10% valley definition). Electron impact (EI) was used wherever feasible with an ionization voltage of 70 eV and perfluorokerosene as a calibrant. Fast atom bombardment (FAB) was performed in a 3-nitrobenzyl alcohol matrix vs a poly(ethylene glycol) calibrant when EI did not give a substantial parent ion signal.

The majority of the fluorescence spectra were recorded on a spectrofluorometer equipped with double-grating excitation and emission monochromators, a 450 W xenon arc lamp source, and a thermoelectrically cooled photomultiplier tube detector and were continuously corrected for fluctuations in excitation intensity by using a Rhodamine-B reference quantum counter. Corrections for PMT response were applied to all spectra based on calibration with a standard lamp according to the manufacturer's instructions.

Analytical gas chromatography was performed on a chromatograph equipped with a Hewlett-Packard Ultra-2 (5% phenyl/methyl polysiloxane) capillary column (~15 m × 0.25 mm × 0.32 μm film thickness).

High-performance liquid chromatography (HPLC) was performed using a PAH Hypersil 150 mm × 3 mm × 5 mm reverse-phase column, maintained at 15 °C. Elution (2 mL/min) was according to the following gradient: 25% water/75% methanol maintained for 5 min and then ramped to 10% water/90% methanol over 25 min. After 0.1 min at the final eluent concentration, the column was flushed with 100% THF to elute any polymer residue for 8 min, after which the column was reequilibrated with 25% water/75% methanol for 8 min prior to the next injection. Typical injection volumes were 3 μL, and detection was by diode-array UV−vis spectrum with integration at individually selected wavelengths for each analyte of interest.

Optical bench experiments were performed on an apparatus consisting of an Oriel 68805 200 W universal power supply powering an Oriel 66002 research lamp housing with integral collimator assembly equipped with an Oriel 6283 200 W Hg lamp mounted to an Oriel 11150 high-stability optical rail. Connected in series to the collimator assembly (kept fully defocused) of the lamp housing was an Oriel 71430 manual shutter, an Oriel 6194 liquid filter kept charged with deionized water, and an Oriel 77660 flanged holder containing a frosted quartz diffusing element (Edmund Industrial Optics, part no. F-32406). Also mounted to the rail were two Oriel 11680 rail mounts. The first rail mount held an Oriel 12730 post-mounted 2 in. filter holder that contained the filters used to select a single mercury line: a Schott GG-395 long-pass cutoff filter followed by an Oriel 56541 interference filter for 405 nm irradiations or a Schott WG-335 long-pass cutoff filter followed by an Oriel 56521 interference filter for 334 nm irradiations. Solutions used for chemical actinometry were placed in an Oriel 13950 1 cm cuvette holder, which held the interior front face of a standard 1 cm cuvette flush with the mounting post. The front face of the cuvette holder was equipped with a black-anodized aluminum light shield containing a 1.45 cm^2 aperture (0.85 × 1.70 cm) that was centered on the output beam of the lamp. Film samples were mounted between aluminum plates (vide infra) in a Thor Labs FP01 sample holder that was modified to accept an Oriel post so that the film plane was flush with the mounting post.

Size exclusion chromatography (SEC) was performed with uninhibited tetrahydrofuran (THF) (with 0.2% acetone added to the injection solvent as a flow marker to correct the nominal 1.0 mL/min flow rate) using three Polymer Laboratories 7.5 mm × 300 mm PLgel mixed-C columns, calibrated with narrow molecular weight distribution polystyrene standards between molecular weight 580 and 2 300 000, enabling determination of number-average (M_n), weight-average (M_w), and *z*-average (M_z) molecular weights (corrected for axial dispersion assuming a Gaussian band-broadening function, when appropriate), as well as polydispersity index (PDI = M_w/M_n) and intrinsic viscosity (dL/g) in THF at 30 °C. The detectors, arranged in series, were a Waters 2487 Spectroflow spectrophotometric detector (UV), a Precision Detectors PD2000 light-scattering (LS) detector operating at 15° and 90°, a Viscotek H502A differential viscometer (DV), and a Waters 410 differential refractive index (DRI) detector. The columns, LS, DV, and DRI detector temperatures were maintained at 30 °C. Polystyrene (PS) equivalent molecular weights are reported.

A TA Instruments model 2920 differential scanning calorimeter (DSC) was used either with a standard heating mode (linear temperature ramp) or modulated temperature mode (sinusoidal T-modulation imposed on linear T-ramp) to determine glass transition temperature (T_g) values. A nitrogen purge (50 mL/min) was used unless small molecule dopants were present. Heating rates were 10 °C/min for standard DSC or 5 °C/min for modulated DSC (with modulation amplitude of 0.531 °C and 40 s modulation period, used to enhance weak transitions, especially at lower temperatures). T_g values reported are at the step-transition midpoint. Typically, results of a second heat are reported, unless an exotherm corresponding to significant isomerization of pendant moieties was observed above T_g or when trying to ascertain the T_g of a polymer with dissolved volatile small molecules. The sample size was typically 10−15 mg, and if dopants were present, a hermetically sealed aluminum pan was employed to prevent loss of volatiles during heating.

Transmission electron microscopy (TEM) was performed on polymer samples coated on the ESTAR Base. The film samples were mounted in a microtome, and thin (≈0.1 μm) sections were prepared. These sections were transferred to a copper grid with a carbon-coated Formvar film and examined in an FEI CM 20 transmission electron microscope. The sections were examined in a cooling holder at liquid nitrogen temperatures to minimize beam damage to the samples.

Di-*tert*-amyl Phthalate. A 500 mL round-bottomed flask was fitted with a Soxhlet extractor containing a disposable cellulose thimble filled with 45 g of Linde 4 Å activated molecular sieves. The flask was charged with 25 mL of 0.2 M potassium *tert*-amoxide in *tert*-amyl alcohol, 200 mL of benzene, and 8.06 g (41.5 mmol) of dimethyl phthalate, and the reaction mixture was brought to reflux under a nitrogen atmosphere. Additional 0.2 M potassium *tert*-amoxide in *tert*-amyl alcohol (10 mL) was added after 40 and 90 h. After 110 h, the reaction vessel was cooled to room temperature, and the reaction mixture was transferred to a separatory funnel containing 100 mL of water and 50 mL of hexane. The layers were separated, and the organic layer was washed with water and brine and dried over anhydrous sodium carbonate. Vola-

tiles were removed by rotary evaporation, and the residue was further concentrated in vacuo (ca. 0.5 mmHg) with gentle warming to give 11.5 g of a light yellow oil that was distilled (bp 127 °C, 0.7 mmHg) to give 9.6 g (76%) of a viscous, clear, colorless oil. ^{1}H NMR ($CDCl_3$): δ 7.64 (m, 1.94 H), 7.47 (m, 1.96 H), 1.91 (q, 3.99 H), 1.58 (s, 12.21 H), 0.96 (t, 5.90 H). ^{13}C NMR ($CDCl_3$): δ 166.8, 133.9, 130.4, 128.8, 84.4, 33.7, 25.5, 8.4. Exact mass (FAB-HRMS), $C_{18}H_{27}O_4$ (M + H): calculated 307.1909, found *m/z* 307.1891. DSC: $T_g = -64$ °C, T_c(onset) = 1 °C, T_m(onset) = 23 °C.

MMA Polymerization with and without 3. Two test tubes were each charged with 0.0138 g of 2,2′-azobis(isobutyronitrile) (AIBN) (0.084 mmol) and 2 mL (1.872 g, 18.7 mmol) of methyl methacrylate (MMA). To one tube was added 0.120 mL (0.0964 g, 0.594 mmol) of **3**. Both tubes were sealed with septa and the contents vigorously purged with nitrogen for 10 min. The tubes were then immersed in an oil bath maintained at 65 °C for 24 h. The tubes were broken, and the hard, glassy polymers in each were dissolved in 15 mL of dichloromethane with sonication. A portion of each solution was precipitated into vigorously stirred methanol and dried in a vacuum oven at 80 °C for 2 h. ^{1}H NMR analysis showed the polymers to be indistinguishable. Molecular weight determinations were made by size exclusion chromatography. Polymer prepared in the presence of **3** gave $M_n = 145\,000$, $M_w = 537\,000$, and PDI = 3.71. Polymer prepared in absence of **3** gave $M_n = 278\,000$, $M_w = 771\,000$, and PDI = 2.77. T_gs for both polymer samples were indistinguishable (127 °C), as were the transition enthalpies 0.047 W/g.

The recovery of **3** was determined by repeating the polymerization of MMA in the presence of **3** in a fashion identical to that described above. The resulting hard, glassy polymer was dissolved in dichloromethane containing an internal standard (adamantane). The solution was analyzed by gas chromatography, and the response factor-corrected percentage of **3** remaining was found to be 98%.

Preparation of 6. A three-necked flask equipped with an addition funnel, nitrogen inlet, and rubber septum was charged with 34.2 g (256 mmol) of aluminum chloride, 140 mL of dry dichloromethane, and a magnetic stir bar. The flask was immersed in an ice−water bath, and 26.3 g (486 mmol) of 2-butyne in 70 mL of dry dichloromethane was slowly added via the addition funnel. The reaction mixture was stirred for 20 min and then transferred via Teflon cannula into a solution of 20.1 g (179 mmol) of ethyl 2-butynoate in 70 mL of dry dichloromethane maintained at 0 °C. The resultant deep red-brown clear solution was stirred for 15 min at 0 °C, and then a solution of 70 mL of dimethyl sulfoxide (DMSO) and 170 mL of dichloromethane was added slowly via an addition funnel. The reaction mixture was stirred for 45 min and then poured into 500 mL of ice−water. The resulting mixture was twice extracted with pentane, and the combined organic extracts were successively washed with water and brine and then dried over anhydrous sodium sulfate. The solvent was removed by rotary evaporation to give 46 g of a clear, light orange oil that was vacuum-distilled (63−67 °C/0.03−0.05 mmHg) to give 28.5 g (72%) of a colorless oil. ^{1}H NMR ($CDCl_3$): δ 4.20 (q, 2.01 H), 2.05 (s, 3.09 H), 1.65 (s, 3.22 H), 1.60 (s, 2.95 H), 1.30 (t, 2.95 H), 1.25 (s, 2.95 H), 1.20 (s, 2.82 H). ^{13}C NMR ($CDCl_3$): δ 168.6, 164.5, 145.5, 141.9, 138.4, 59.3, 56.9, 54.7, 14.5, 14.2, 11.3, 11.1, 10.7. Exact mass, $C_{14}H_{20}O_2$: calculated 220.1464, found *m/z* 220.1449. This procedure is analogous to that reported for the methyl ester.[17]

Preparation of 7. To 26.0 g (118 mmol) of ester **6** in 500 mL of dry ether at 0 °C under nitrogen was added 250 mL (250 mmol) of a 1.0 M solution of diisobutylaluminum hydride in hexanes over 40 min. The reaction mixture was stirred 1 h at 0 °C and 2 h at room temperature. The mixture was cooled in an ice bath, and 11 mL (8.7 g, 270 mmol) of methanol was slowly added. A saturated aqueous solution (200 mL) of sodium sulfate was added, plus an additional 100 mL of ether. Anhydrous magnesium sulfate was added until a granular precipitate formed. The mixture was filtered, and the precipitate was washed with dry ether. The combined filtrate was concentrated to give a pale yellow oil that slowly crystallized. Recrystallization from hexanes yielded 13.0 g (62%) of a white crystalline solid; mp 57−58.5 °C. ^{1}H NMR ($CDCl_3$): δ 4.15 (2 dd, 2H), 1.70 (s, 3.06 H), 1.64 (s, 2.99 H), 1.61 (s, 2.98 H), 1.18 (s, 3.05 H), 1.14 (s, 2.99 H), 1.10 (t, 0.94 H). ^{13}C NMR ($CDCl_3$): δ 148.2, 146.3, 144.6, 143.5, 57.9, 56.0, 54.8, 11.9, 11.6, 11.3, 10.9, 10.1. Exact mass, $C_{12}H_{18}O$: calculated 178.1358, found *m/z* 178.1358. While this compound has been previously reported,[27] its characterization has not.

Preparation of 5. To a solution of 5.80 g (32.5 mmol) of alcohol **7**, 6.20 mL (4.50 g, 44.5 mmol) of triethylamine, 0.210 g (1.72 mmol) of 4-dimethylaminopyridine, and 20 mg of bis(3-*tert*-butyl-4-hydroxy-5-methylphenyl) sulfide in 110 mL of dry dichloromethane stirring under nitrogen was added dropwise 3.30 mL (3.50 g, 33.8 mmol) of methacryloyl chloride. After addition was complete, the reaction mixture was heated to reflux for 2.5 h. After cooling to room temperature, the reaction mixture was diluted with 200 mL of ether, successively washed with water, saturated aqueous sodium bicarbonate, 1 M aqueous sodium hydroxide, water, and brine. The organic phase solution was dried over anhydrous sodium sulfate, and solvent was removed by rotary evaporation to give a clear yellow oil. Vacuum distillation (63 °C, 0.05 mmHg) gave 7.05 g (88%) of a clear colorless oil. ^{1}H NMR ($CDCl_3$): δ 6.15 (s, 0.99 H), 5.60 (s, 0.99 H), 4.66 (br s, 1.99 H), 2.00 (s, 2.93 H), 1.75 (s, 3.04 H), 1.61 (s, 3.00 H), 1.60 (s, 2.98 H), 1.18 (s, 3.05 H), 1.15 (s, 3.03 H). ^{13}C NMR ($CDCl_3$): δ 167.5, 150.5, 144.5, 143.2, 141.8, 136.7, 125.4, 59.8, 56.2, 55.0, 18.6, 12.0, 11.4, 11.2, 10.9, 10.0. Exact mass, $C_{16}H_{22}O_2$: calculated 246.1621, found *m/z* 246.1624. This compound was routinely stored over a few milligrams of inhibitor, bis(3-*tert*-butyl-4-hydroxy-5-methylphenyl) sulfide. The inhibitor was removed by passage of the monomer through a short column of basic alumina prior to use.

Preparation of Functionalized Copolymers. p(DBMA/MMA). A solution of 4.29 g (17.4 mmol) of **5**, 15.7 g (157 mmol) of methyl methacrylate, and 0.85 g (4.42 mmol) of Vazo-67 [2,2′-azobis(isovaleronitrile)] in 100 mL of chlorobenzene was deaerated by sparging with nitrogen for 10 min and then heated at 65−70 °C for 24 h. The resulting polymer was precipitated into excess methanol, subsequently dissolved in dichloromethane, and reprecipitated into excess methanol. The polymer was collected and dried overnight at 80 °C in a vacuum oven to give 11.6 g of p(DBMA/MMA). The mole ratio of Dewar benzene to methyl methacrylate monomer units present in the copolymer was determined to be ≈1:9 by ^{1}H NMR spectroscopy by integration of the resonances at δ 4.4 ppm (Dewar benzene, allylic ester methylene) and 3.6 ppm (methyl ester). The molecular weight distribution of the copolymer was measured by SEC against polystyrene standards in tetrahydrofuran solvent. $M_n = 27\,100$; $M_w = 46\,900$; PDI = 1.73. The glass transition temperature (T_g) was found to be 115 °C by differential scanning calorimetry performed in a nitrogen atmosphere at a heating rate of 10 °C/min.

p(DBMA/HMA). An analogous procedure using 2.11 g (8.57 mmol) of **5**, 12.90 g (75.77 mmol) of *n*-hexyl methacrylate, and 0.41 g (2.13 mmol) of Vazo-67 in 75 mL of chlorobenzene gave 6.9 g of copolymer. $M_n = 19\,800$; $M_w = 44\,000$; PDI = 2.22; T_g = 4 °C.

p(DBMA/cHMA). An analogous procedure using 0.99 g (4.02 mmol) of **5**, 6.11 g (36.3 mmol) of cyclohexyl methacrylate, and 0.38 g (1.98 mmol) of Vazo-67 in 75 mL of chlorobenzene gave 6.2 g of copolymer. $M_n = 12\,900$; $M_w = 43\,500$; PDI = 3.37; $T_g = 106$ °C.

Preparation of Polymer Films. Dichloromethane solutions of polymers were knife-coated using a 0.005 in. drawbar style coating knife on ESTAR Base sheets. Solutions typically contained ≈1 g of polymer in ≈4 mL of dichloromethane, variable amounts of sensitizer and reactant (for molecularly doped samples), and plasticizer. All solutions were filtered through Centrex MF-5 (0.45 μm nylon membrane) centrifugal filter tubes before coating. For quantum yield measurements on functionalized polymer films, di-*tert*-amyl phthalate was most commonly used as a plasticizer because it permitted more accurate integration of NMR signals at low conversion. The ESTAR Base support was mounted on an

aluminum coating block that was maintained at 23−25 °C by a circulating water bath. The coating block had a hinged cover that was closed to protect the coating while air-drying. After drying on the coating block for 10−20 min, the coatings were cut into individual films using a rotary blade paper trimmer. These films were mounted between two 50 mm × 60 mm × 1/16 in. aluminum plates. The plates had a 23 mm wide × 6 mm deep notch cut in the bottom (50 mm) edge, which fit into a Thor Labs FP01 sample holder used for photolysis experiments. The plates also contained a 1 in. or a 1.5 in. diameter aperture that was centered 30 mm above the top of the notch. Mounted films were dried in vacuo (0.01 mmHg) at either 75−80 °C for 1.5 h or room temperature for 12−16 h. Both sets of drying conditions were demonstrated to leave ≤1.5 wt % residual dichloromethane in the polymer films by ^{1}H NMR analysis vs an internal standard. Under the latter drying conditions, the thermal isomerization of **1** to **2** in films was typically <4%. Dried coatings had an ultimate thickness of ≈20 μm. After drying, films were examined by UV−vis spectroscopy in multiple locations at the λ_{max} of the sensitizer to test uniformity of the film thickness. Only films with OD variations of <5% were used. Coatings on glass were prepared in a similar manner.

Fluorometry. The fraction of sensitizer-excited states intercepted (quenched) by reactant molecules was determined by fluorometry. Film samples with similar optical density and sensitizer concentration, with and without quencher, were cut out by using a 1.5 in. arch punch and mounted between two 1.5 in. diameter quartz disks in Newport LH-150 mounts. The mounts were secured in the spectrofluorometer with a home-built stage. Spectra were recorded in front-face mode, and samples were excited at the same wavelength used for optical bench irradiations. The emission spectrum of an identically mounted film of ESTAR Base was used to background correct all emission spectra.

Quantum Yield Measurements. Irradiations for quantum yield determinations were done on the optical bench in an air atmosphere. The photon flux was determined using phenanthrenequinone and 1 mM *trans*-stilbene in benzene[28] for 405 nm irradiations and Aberchrome 540 (ca. 5 mM on toluene)[29] for 334 nm irradiations. Irradiated films were prepared for analysis by GC or NMR to determine the molecules of product formed by photolysis as follows. The portion of the film that had been irradiated through the 1 in. aperture of the aluminum plates was marked with a metal scribe using the aluminum plate as a guide. The film was removed from between the metal plates, and an area within the scribed region was cut out with a 15/16 in. arch punch. The polymer film was cut in half and placed into a scintillation vial. For polymer films containing molecularly doped cage compound **1** samples, 0.7 mL of a $CDCl_3$ solution containing 1,3,5-trioxane as internal standard was added, and the vial was sonicated for 10 min and then allowed to stand 20−30 min with occasional swirling. The solution was pipetted away from the Estar film into amber-colored NMR tubes. The numbers of molecules of **1** and **2** (integrating the four bridgehead methyne signals for each) were determined vs the known number of molecules of trioxane by ^{1}H NMR integration. For polymer films containing molecularly doped **3**, 0.4 mL of dichloromethane and a known amount of *n*-tetradecane as internal standard were added to the vial. The vial was sonicated for 15 min, and then 1.4 mL cyclohexane was added to precipitate the polymer. The mixture was filtered and the solution analyzed by gas chromatography to determine the GC response factor corrected number of molecules of **3** and **4** present. Functionalized polymer samples were analyzed as for those containing **1** except 1,1,2,2-tetrabromoethane was used as an internal standard. Sufficiently long delay times were used in the NMR experiments to ensure complete relaxation of nuclei between rf pulses.

The reported quantum yields are corrected for the fraction of incident light absorbed by the samples and for the fraction of excited states that were quenched, as determined by fluorometry (vide supra).

Conversion Experiments. Irradiation of films for conversion experiments were done in a similar manner for quantum yield measurements except for films containing molecularly doped **3**. Irradiations of these latter films were performed under a nitrogen atmosphere in a home-built purge cell to minimize loss of **3/4** that occurred upon prolonged irradiation in air. The fractional conversion of reactants was determined as described for the quantum yield measurements.

Control Experiment with 1/Ferrocene/PMMA. Polymer films containing 0.5 M **1** and 0.6 M ferrocene in PMMA were prepared as described above. The films were irradiated at 405 nm, and the extent of conversion was determined by ^{1}H NMR using 1,3,5-trioxane as an internal standard, as described earlier. For a photon radiant energy (i.e., number of photons absorbed) that resulted in ≈30% conversion of **1** to **2** with DCA as photosensitizer, films with **1**/ferrocene showed <1% isomerization (four repetitions).

Forced Rayleigh Scattering Experiments. Experiments were conducted with polymer films coated on glass using an optical table equipped with air suspension legs to provide vibration isolation. Irradiation was provided by a krypton ion laser operating at 407 nm. The laser light was spatially filtered using a UV-grade 0.25 NA microscope objective and a 10 μm diameter pinhole held by a Optosigma 118-0910 spatial filter mount. The spatially filtered light was collimated using a 50 mm focal length, 1 cm diameter plano-convex lens. The collimated beam was split by a 1 × 2 cm Stocker-Yale Lasiris phase mask (1060.02 ± 0.02 nm grating optimized for first-order diffraction at 400 nm). The first-order beams were crossed at the axis of a computer-controlled rotation stage. The sample was mounted in a Thor Labs FP01 sample holder so as to hold the film plane at the center of the rotation axis. The angle of interference (35.55° from normal) and the wavelength of the laser defined the grating period (350 nm). Grating formation was monitored with 632.8 nm light from a helium−neon (HeNe) laser (∼10 mW). The HeNe laser light was chopped at ≈210 Hz using a Stanford Research Systems SR540 chopper wheel and frequency controller. The HeNe probe beam was Bragg matched to the grating (incident at 64.7° from normal), and the diffracted beam was monitored using a large area (0.43 in. diameter active area) silicon detector that was interfaced to a personal computer via a lock-in amplifier set to the chopper frequency.

After writing the diffraction grating, the sample was transferred to a second computer-controlled sample holder/rotation stage assembly and mounted for long-term monitoring. The HeNe beam was switched from one stage to the other with a manual flip mirror. The sample and rotation state were covered with a light-tight box that contained two small openings to allow the probe light in and out. During long-term monitoring the HeNe incident intensity (I_{inc}) was monitored as well as the diffracted intensity (I_{diff}). I_{diff}/I_{inc} was measured to correct for any fluctuations in HeNe source intensity. Switching from measurement of incident to diffracted light intensity was computer-automated by using a New Focus 8891 electromechanical flip mirror. A custom-built switch box was used to switch between output of incident or diffracted beam detector to the lock-in amplifier. Data were collected and averaged over 2 min for each detector every 30 min for as long as desired, typically several weeks. Between data collections, the motorized flip mirror was positioned to block the sample from the HeNe beam.

Acknowledgment. Research support was provided by the National Science Foundation (DMR-0071302) and, in part, by the Center for Electronic Imaging Systems (CEIS), a NYSTAR-designated Center for Advanced Technology. We thank Thomas H. Mourey and Kim Le for SEC measurements; Michael R. Landry and Roger E. Moody for DSC measurements; Thomas C. Jackson for high-resolution MS measurements; Donald L. Black, Theodore R. Van Dam, and Stephen C. Stoker for TEM imaging; and Tamara F. Marchinsin and

Timothy C. Schunk for HPLC methods development, all members of Kodak R&D laboratories. We are grateful to Ralph H. Young (University of Rochester) for numerous instructive and enlightening discussions. We are also pleased to acknowledge valuable advice and encouragement from Jack C. Chang (Eastman Kodak Company).

References and Notes

(1) Taken in part from the Ph.D. Thesis of Jason G. Gillmore, University of Rochester, New York, 2003.

(2) (a) Fyson, J. R.; Twist, P. J.; Gould, I. R. In *Electron Transfer in Chemistry: Molecular-level Electronics, Imaging and Information, Energy and the Environment*; Balzani, V., Ed.; Wiley-VCH: New York, 2001; Vol. 5, p 285. (b) West, W.; Gilman, P. B. In *The Theory of the Photographic Process*, 4th ed.; James, T. H., Ed.; MacMillan: New York, 1977; p 251. (c) Borsenberger, P. M.; Weiss, D. S. *Organic Photoreceptors for Xerography*; Marcel Dekker: New York, 1988.

(3) (a) Crivello, J. V. *NATO Sci. Ser., Ser. E: Appl. Sci.* **1999**, *359*, 45. (b) Belfield, K. D., Crivello, J. V., Eds.; *Photoinitiated Polymerization*; ACS Symposium Series 847; American Chemical Society: Washington, DC, 2003. (c) Fouassier, J. P., Rabek, J. F., Eds.; *Radiation Curing in Polymer Science and Technology*; Elsevier: New York, 1993.

(4) (a) Stewart, M. D.; Patterson, K.; Somervell, M. H.; Willson, C. G. *J. Phys. Org. Chem.* **2000**, *13*, 767. (b) Reiser, A. *Photoreactive Polymers*; Wiley: New York, 1989.

(5) See, for example: (a) Evans, T. R.; Wake, R. W.; Sifain, M. M. *Tetrahedron Lett.* **1973**, 701. (b) Okada, K.; Hisamitsu, K.; Mukai, T. *Tetrahedron Lett.* **1981**, 1251. (c) Crellin, R. A.; Lambert, M. C.; Ledwith, A. *J. Chem. Soc., Chem. Commun.* **1970**, 682. (d) Majima, T.; Pac, C.; Sakurai, H. *Chem. Lett.* **1979**, 1133. (e) Jones, G., II.; Becker, W. G.; Chiang, S.-H. *J. Photochem.* **1982**, *19*, 245. (f) Borsub, N.; Kutal, C. *J. Am. Chem. Soc.* **1984**, *106*, 4826. (g) Stufflebeme, G.; Lorenz, K. T.; Bauld, N. L. *J. Am. Chem. Soc.* **1986**, *108*, 4234. (h) Bauld, N. L. *Tetrahedron* **1989**, *45*, 5307. (i) Nelsen, S. F. *Acc. Chem. Res.* **1987**, *20*, 269. (j) Tamai, T.; Ichinose, N.; Tanaka, T.; Sasuga, T.; Hashida, I.; Mizuno, K. *J. Org. Chem.* **1998**, *63*, 3204.

(6) Robello, D. R.; Dinnocenzo, J. P.; Farid, S.; Gillmore, J. G.; Thomas, S. W., III In *Chromogenic Phenomena in Polymers*; Jenekhe, S. A., Kiserow, D. J., Eds.; ACS Symposium Series 888; American Chemical Society: Washington, DC, 2004; p 135.

(7) (a) Hasegawa, E.; Okada, K.; Mukai, T. *J. Am. Chem. Soc.* **1984**, *106*, 6852. (b) Hasegawa, E.; Okada, K.; Ikeda, H.; Yamashita, Y.; Mukai, T. *J. Org. Chem.* **1991**, *56*, 2170.

(8) Mukai, T.; Yamashita, Y. *Tetrahedron Lett.* **1978**, 357.

(9) Van Haver, Ph.; Viaene, L.; Van der Auweraer, M.; De Schryver, F. C. *J. Photochem. Photobiol. A: Chem.* **1992**, *63*, 265.

(10) (a) Taylor, G. N. *Z. Phys. Chem. (Wiesbaden)* **1976**, *101*, 237. (b) Jones, G., II.; Chiang, S.-H. *J. Am. Chem. Soc.* **1979**, *101*, 7421. (c) Jones, G., II.; Chiang, S.-H. *Tetrahedron* **1981**, *37*, 3397. (c) Jones, G., II.; Becker, W. G. *J. Am. Chem. Soc.* **1983**, *105*, 1276.

(11) Kiau, S.; Shukla, D.; Farid, S.; Young, R.; Dinnocenzo, J. P., manuscript in preparation.

(12) Cf. (a) Hervet, H.; Urbach, W.; Rondelez, F. *J. Chem. Phys.* **1978**, *68*, 2725. (b) Lodge, T.; Chapman, B. *Trends Polym. Sci.* **1997**, *5*, 122. (c) Yu, H. *Polym. Prepr.* **1991**, *32*, 398.

(13) The diffusion coefficient (D) is equal to $(\Lambda^2/8\pi^2 t)\ \ln(I_0/I_t)$, where Λ is the grating period, I_0 is the initial diffraction efficiency, and I_t is the diffraction efficiency at time t (ref 12).

(14) PC Model, ver. 8.5, Serena Software.

(15) Smoluchowski, M. V. *Z. Phys. Chem.* **1917**, *92*, 129.

(16) Berens, A. R.; Hoppenberg, H. B. *J. Membr. Sci.* **1982**, *10*, 283.

(17) (a) Dopper, J. H.; Greijdanus, B.; Oudman, D.; Wynberg, H. *Tetrahedron Lett.* **1975,** *48*, 4297. (b) van Rantwijk, F.; Timmermans, G. J.; van Bekkum, H. *Pays-Bas* **1976**, *95*, 39.

(18) Greenley, R. Z. In *Polymer Handbook*, 4th ed.; Brandrup, J., Immergut, E. H., Grulke, E. A., Eds.; Wiley: New York, 1999; pp II/181−308.

(19) Glass transition temperatures were generally experimentally determined but could be accurately estimated from the weight fractions of the polymer components. See: Cowie, J. M. G. *Polymers: Chemistry & Physics of Modern Materials*; Chapman & Hall: New York, 1991; p 327.

(20) (a) Perrin, F. *C. R. Acad. Sci. Paris* **1924**, *178*, 1978. (b) Frank, I. M.; Vavilov, S. I. *Z. Phys.* **1931**, *69*, 100. (c) Perrin, F. *Ann. Chem. Phys.* **1932**, *17*, 283. (d) Lakowicz, J. R. *Principles of Fluorescence Spectroscopy*, 2nd ed.; Kluwer: New York, 1999; Chapter 8.

(21) ϕ_0/ϕ was found to increase slightly with increasing [DCA]. This observation can reasonably be ascribed to the intervention of Förster energy transfer at high [DCA]. Excited DCA molecules that lack a molecule of **1** in their quenching sphere are more likely to undergo Förster energy transfer with neighboring, ground-state DCA molecules as [DCA] increases. This will lead to a decrease in the fluorescence quantum yield (ϕ) with increasing [DCA] and an increase in ϕ_0/ϕ. Since application of eq 8 requires a value of ϕ_0/ϕ that is uncontaminated by any contribution from Förster energy transfer, the value of ϕ_0/ϕ was determined for 0.5 M **1** in PMMA from plot of ϕ_0/ϕ vs [DCA] by extrapolation to [DCA] = 0.

(22) Quantum yields for cation radical chain isomerization of **3** are generally greater than those for **1**; cf. refs 5a and 5b.

(23) These reductions potentials were measured in a polar solvent and may not reflect the potentials in a polymer medium.

(24) (a) Sah, R. E.; Baur, G.; Kelker, H. *Appl. Phys.* **1980**, *23*, 369. (b) Eisenbach, C. D.; Sah, R. E.; Baur, G. *J. App. Polym. Sci.* **1983**, *28*, 1819.

(25) (a) Pangborn, A. B.; Giardello, M. A.; Grubbs, R. H.; Rosen, R. K.; Timmers, F. J. *Organometallics* **1996**, *15*, 1518. (b) Alaimo, P. J.; Peters, D. W.; Arnold, J.; Bergman, R. G. *J. Chem. Educ.* **2001**, *78*, 64.

(26) Dockery, K. P.; Dinnocenzo, J. P. Farid, S.; Goodman, J. L.; Gould, I. R.; Todd, W. P. *J. Am. Chem.* Soc. **1997**, *119*, 1877.

(27) Gorycki, P. D.; Macdonald, T. L. *Chem. Res. Toxicol.* **1994**, *7*, 745.

(28) (a) Bohning, J. J.; Weiss, K. *J. Am. Chem. Soc.* **1966**, *88*, 2893. (b) Brown-Wensley, K. A.; Mattes, S. L.; Farid, S. *J. Am. Chem. Soc.* **1978**, *100*, 4162.

(29) (a) Hatchard, C. G.; Parker, C. A. *Proc. R. Soc. London, Ser. A* **1956**, *235*, 518. (b) Heller, H. G.; Langan, J. R. *J. Chem. Soc., Perkin Trans. 2* **1981**, 341.

MA050348K